A Novel Method for Measuring Shield Tunnel Cross Sections

Ya-dong Xue[1,2(✉)], Sen Zhang[1,2], and Zhe-ting Qi[2]

[1] Key Laboratory of Geotechnical and Underground Engineering of Education Ministry, Tongji University, Shanghai 200092, China
yadongxue@126.com
[2] Department of Geotechnical Engineering, Tongji University, Shanghai 200092, China

Abstract. With more metro tunnels being constructed and operated, the task of measuring tunnels' deformation becomes more imperative. This article proposes a novel method for measuring shield tunnel cross sections based on close range photogrammetry. Direct Linear Translation (DLT) method is suitable for non-metric photography, requiring several control points on the linings, which is time-consuming. A new method of setting control points was put forward to overcome the shortcoming. A laser source forms a bright outline on the tunnel's inner surface. The polar coordinates of control points on the outline are gained by a laser range-finder installed on a 360° protractor. These coordinates are used to solve the unknown parameters of DLT equations. Then the precise outline of the tunnel cross sections can be obtained. A series of tests in the subway tunnel of Shanghai Metro Line 1 were carried out to validate the method being precise and effective.

Keywords: Tunnel lining deformation · Cross sections
Close range photogrammetry · Laser orientation · Laser range-finding

1 Introduction

With a large number of metro tunnels being constructed and operated in China, the fast and effective tunnel deformation measuring method becomes imperative as tunnel's deformation condition is important for evaluating its performance. Most of the metro tunnels are constructed using the shield method. Shield tunnels' deformation is generally induced by cyclic train loads, foundation deformation and adjacent construction activities, not only impacting tunnels' durability but also reducing their safety factors (Wang et al. 2009) [1]. In soft soil regions such as Hangzhou city and Shanghai city, tunnels' deformation is usually large. The maximum deformation observed in Shanghai metro was 148 mm (2.4%D) (Zhang et al. 2014) [2].

Traditional deformation measuring techniques mainly include Bassett convergence instruments and total stations. The convergence instruments, which measure tunnels' deformation through the change of the measuring lines' length, are typical contacting measurements. Setting an enormous number of measuring lines is time-consuming, costly and tedious (Bassett et al. 1999) [3]. Measurement of total station is discrete and

Y. Zhao et al. (Eds.): ICIG 2017, Part III, LNCS 10668, pp. 47–57, 2017.
https://doi.org/10.1007/978-3-319-71598-8_5

inflexible even though it implements precise and non-contact measurements (Hope et al. 2008; Yang et al. 2005; Yang et al. 2006) [4–6]. These two methods cannot satisfy the increasing measuring requirements any longer due to the shortcomings aforementioned.

Some new measuring methods have appeared in recent years such as light detection and ranging (LiDAR), which is able to obtain the complete data of cross sections. Han et al. (2013) [7] used Minimum-Distance Projection (MDP) algorithm to establish point correspondences to measure tunnels' deformation. Some researchers established 3D models of tunnels using terrestrial laser scanning to measure tunnels' geometry deformation and settlement (Xie et al. 2017; Argüelles et al. 2013) [8, 9], but for most subway companies it's still too expensive.

The close range photogrammetry technology advances rapidly as digital single-lens reflex cameras mature. Study on photogrammetry using non-metric cameras has become a research hotspot during the past years. The shapes, dimensions and locations of the vertical cross-sections of tunnels can be derived from the photographs based on the control data provided by two targets' locations on the plates (Ethrog et al. 1982) [10]. Zhang et al. (2001) [11] used a CCD area array camera to measure areas of irregular plane objects. Yang et al. (2001) [12] proposed a novel algorithm to improve CCD cameras' measuring precision. Lee et al. (2006) [13] found that the displacement and strain data obtained with close range photogrammetric technique in a model tunnel showed a remarkable agreement with the physical data. Hu (2008) [14] used close range photogrammetry to measure a mountain tunnel's deformation, but the precision was unsatisfactory. Chen et al. (2014) [15] proposed using a mobile metal bracket to offer control points, which improved the practicability and maneuverability of DLT method in tunnel engineering.

This article tries to create a novel method for measuring shield tunnel cross sections based on laser orientation, laser range-finding and close range photogrammetry. Based on a novel way of setting control points and target points by using laser, this article studies on how to apply DLT method in tunnel monitoring. A specially-designed device was used in the field experiment. The results proved the practicability and accuracy of the proposed method.

2 Close Range Photogrammetry

2.1 Imaging Principle

The pinhole imaging is the fundamental theory of close range photogrammetry (see Fig. 1).

Based on the similar triangles principle, we have:

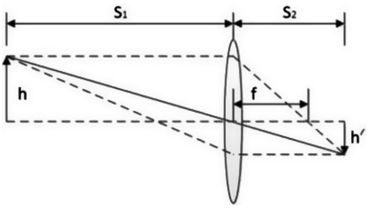

Fig. 1. The theory of pinhole imaging

$$\frac{h}{f} = \frac{h'}{S_2 - f} \tag{1}$$

$$\frac{h}{S_1} = \frac{h'}{S_2} \tag{2}$$

Where h stands for the object height, h' stands for the image height, f represents the focal length, S_1 represents the distance between the object plane and the optical center and S_2 represents the distance between the imaging plane and the optical center.

Rearranging the two equations, we can get:

$$\frac{1}{f} = \frac{1}{S_1} + \frac{1}{S_2} \tag{3}$$

As S_1 is usually far greater than S_2 in engineering projects, it is easy to get:

$$h' = \frac{fh}{S_1} \tag{4}$$

2.2 General Coordinate Systems

Four general coordinate systems are used in DLT method: world coordinate system, camera coordinate system, image coordinate system and pixel coordinate system.

World coordinates are absolute coordinates that objectively describe the three-dimensional space, signified with (X_w, Y_w, Z_w). Camera coordinates are signified with (X_c, Y_c, Z_c) and the origin point of them is located at the lens' optical center. Z_c represents the lens' main optical axis. Image coordinates and pixel coordinates are signified with (x, y) and (u, v) separately. The main difference between them lies in the measurement unit. The former one is measured in millimeter or centimeter whereas the later one is measured in pixel.

Figure 2 shows the conversion relations of the four general systems. It should be pointed out that the conversion between camera coordinates and image coordinates is based on Eq. (4).

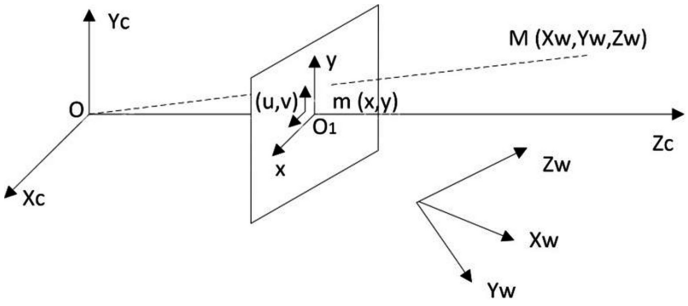

Fig. 2. General coordinate systems

The transformation equation between pixel coordinates and world coordinates is:

$$Z_C \begin{pmatrix} u \\ v \\ 1 \end{pmatrix} = \begin{pmatrix} \frac{1}{d_x} & 0 & u_0 \\ 0 & \frac{1}{d_y} & v_0 \\ 0 & 0 & 1 \end{pmatrix} \begin{pmatrix} f & 0 & 0 & 0 \\ 0 & f & 0 & 0 \\ 0 & 0 & 1 & 0 \end{pmatrix} \begin{pmatrix} R & T \\ 0^T & 1 \end{pmatrix} \begin{pmatrix} X_W \\ Y_W \\ Z_W \\ 1 \end{pmatrix} \tag{5}$$

Where R represents a certain 3×3 rotation matrix and T represents a 3×1 translation matrix. The parameters d_x and d_y are the physical dimensions of one pixel in x-axis direction and y-axis direction in the image plane respectively.

2.3 Direct Linear Translation Method

Among the commonly used parsing methods for close range photogrammetry, DLT is especially suitable for non-metric photography. It does not involve initial approximations for the unknown parameters of inner and outer orientation of the camera (Abdel-Aziz et al. 2015) [16]. DLT contains a direct linear transformation from pixel coordinates into world coordinates with Eq. (6) which is based on Eq. (5).

$$A \cdot m = B \tag{6}$$

$$A = \begin{bmatrix} X_{w1} & Y_{w1} & Z_{w1} & 1 & 0 & 0 & 0 & 0 & -u_1X_{w1} & -u_1Y_{w1} & -u_1Z_{w1} \\ 0 & 0 & 0 & 0 & X_{w1} & Y_{w1} & Z_{w1} & 1 & -v_1X_{w1} & -v_1Y_{w1} & -v_1Z_{w1} \\ X_{w2} & Y_{w2} & Z_{w2} & 1 & 0 & 0 & 0 & 0 & -u_2X_{w2} & -u_2Y_{w2} & -u_2Z_{w2} \\ 0 & 0 & 0 & 0 & X_{w2} & Y_{w2} & Z_{w2} & 1 & -v_2X_{w2} & -v_2Y_{w2} & -v_2Z_{w2} \\ & \vdots & & & & \vdots & & & & \vdots & \\ X_{wn} & Y_{wn} & Z_{wn} & 1 & 0 & 0 & 0 & 0 & -u_nX_{wn} & -u_nY_{wn} & -u_nZ_{wn} \\ 0 & 0 & 0 & 0 & X_{wn} & Y_{wn} & Z_{wn} & 1 & -v_nX_{wn} & -v_nY_{wn} & -v_nZ_{wn} \end{bmatrix}_{2n \times 11} \tag{7}$$

$$B = \begin{bmatrix} u_1 & v_1 & u_2 & v_2 & \cdots & u_n & v_n \end{bmatrix}^T_{2n \times 1} \tag{8}$$

Where m represents the coefficient matrix with Eq. (9). Interior and exterior orientation elements are implicit in the m matrix.

$$m = \begin{bmatrix} m_1 & m_2 & m_3 & m_4 & \cdots & m_{10} & m_{11} \end{bmatrix}^T_{1 \times 11} \tag{9}$$

In general, pixel coordinates in a photo are easily obtained. Then Eq. (6) could be used to calculate the world coordinates of any target point if the m matrix is calculated. To solve the m matrix, several control points are required, of which the world coordinates are known. Three-dimensional DLT method requires at least six control points as there are 11 unknown Parameters in the m matrix. In tunnel engineering, these points are normally set on the inner surface of the linings (Ma et al. 2006) [17]. To improve the measuring precision, they are generally more than six. Actually, it's difficult to set many control points in a shield tunnel, which has restricted the application of DLT method in tunnel projects.

The calculating process of DLT method is divided into four steps: (1) identifying and positioning control points; (2) computing the m matrix (camera calibration); (3) extracting pixel coordinates of target points; (4) calculating world coordinates of target points.

Chen's research is an example of applying DLT method in tunnel engineering (Chen et al. 2014) [15]. A metal bracket was placed in the tunnel with predefined target points on the linings when taking a photo. The bracket established a reference coordinate system in photos. The m matrix could be calculated through these points' coordinates. However, solving any target point needed at least two photos captured from different vision angles because only two equations can be built from one photo for each target point which contains three unknowns: (X_w, Y_w, Z_w).

2.4 Laser-Based Calibration Method

This article proposes a novel calibration method based on laser range-finding, which aims to achieve higher precision at lower cost. A laser source is fixed on a self-made inspection device (MTI-200A) to create a bright outline on the lining surface. On the same device, a laser range-finder is placed on a 360° protractor, which is coplanar with the outline plane (see Fig. 3).

The distances and their corresponding angles of control points are recorded by rotating the laser range-finder (see Fig. 4). The recorded data will be used to calculate world coordinates of control points with Eqs. (10) and (11).

$$X_{wi} = L_i \times sin\theta_i \tag{10}$$

$$Y_{wi} = L_i \times cos\theta_i \tag{11}$$

Where L_i stands for the distance and θ_i stands for the corresponding angle.

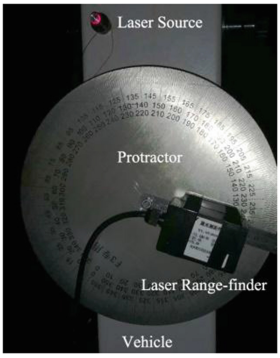

Fig. 3. The related devices

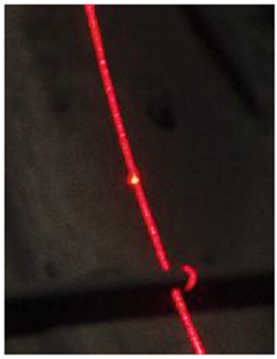

Fig. 4. A control point on the outline

The parameter Z_w in 3D DLT equations is assumed as zero on the hypothesis that the outline and control points are located in the same plane. Then the matrix A in Eq. (7) transforms into 2D form as shown in Eq. (12).

$$A = \begin{bmatrix} X_{w1} & Y_{w1} & 1 & 0 & 0 & 0 & -u_1X_{w1} & -u_1Y_{w1} \\ 0 & 0 & 0 & X_{w1} & Y_{w1} & 1 & -v_1X_{w1} & -v_1Y_{w1} \\ \vdots & \vdots & \vdots & \vdots & \vdots & \vdots & \vdots & \vdots \\ X_{wn} & Y_{wn} & 1 & 0 & 0 & 0 & -u_nX_{wn} & -u_nY_{wn} \\ 0 & 0 & 0 & X_{wn} & Y_{wn} & 1 & -v_nX_{wn} & -v_nY_{wn} \end{bmatrix}_{2n\times 8} \tag{12}$$

Solving the m parameters of 2D DLT requires at least 4 control points due to the unknown number of m has decreased from 11 to 8. To achieve higher measuring precision, more control points are needed. Least squares method as shown in Eq. (13) is used to process the data if there are extra control points.

$$m = (A^TA)^{-1}A^TB \tag{13}$$

The most significant improvement of this method is that solving each target point needs only one photo captured from any vision angle.

The measuring system frame is shown in Fig. 5. The relevant algorithms were programed with Mathematica.

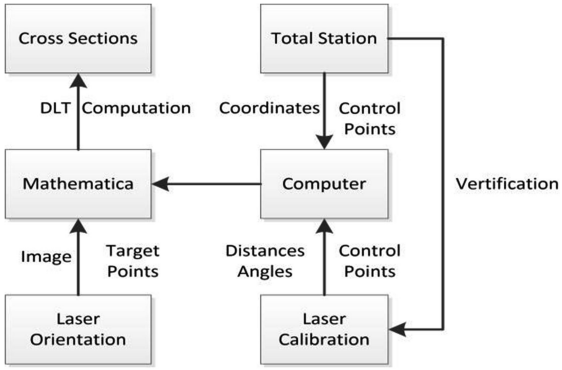

Fig. 5. The measuring system frame

3 Field Test and Verification

3.1 Preparation

The main advantages of non-metric digital cameras are listed as follows: (1) The interior and exterior orientation elements of them can be calculated accurately; (2) They do not need negatives like film cameras do; (3) They storage data in digital form and that data can be easily taken use of by a computer; (4) They are fairly cheaper than

metric cameras. (5) Specially-designed programs are able to complete the calculating process automatically and correctly.

Nikon D7000 digital camera and Tokina AT-X PRO SD 11-16 F2.8 IF DX IINikon lens were chosen as the test equipment as shown in Fig. 6. Full frame cameras were not considered as they had not been in widespread use. The image sensor of D7000 has sixteen million pixels, which is enough for the experiments. A wide-angle lens was required and Tokina 11–16 met the requirements perfectly. The 11 mm focus was preferred because it allowed the experimenter to approach closer to the outline than the 16 mm focus.

The only problem lied in the noticeable barrel image distortion at the 11 mm focus as shown in Fig. 7, released by the famous image quantity reference website DXOMARK [18]. Distortion means that the original straight lines are distorted into curved lines which will undoubtedly lead to some errors in measurements. To avoid that, the Adobe software Lightroom was used to correct the distortion. Figure 8 shows the original image of a gridding board shot by D7000 and Fig. 9 shows the modified image using the Lightroom software. Although the distortion in the image edges is still detectable, the maximum deviation of straight lines has decreased from 75 pixels to 15 pixels. Furthermore, the outline range seldom ever appears on the image edges as Fig. 10 shows, in fact.

In terms of correcting distortion, lots of papers talked about different correcting algorithms. For example, Jin et al. (2011) [19] used BP neural network model to correct image distortion.

Fig. 6. The D7000 camera

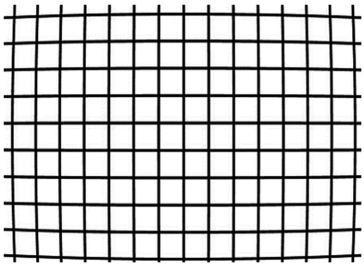

Fig. 7. The image distortion

To demonstrate the feasibility of DLT method, four randomly selected points E, F, G, H in Fig. 9 were chosen as control points to solve the relative coordinates of other points. Each little square was 17.5 mm in width and 24.8 mm in height. The maximum error appeared at the point S which was 1.1315 mm. The pixel distances between target points and the image center were defined as PD. The percentage errors were defined as absolute errors divided by measuring distances. Then the curves of PE in x-axis and y-axis to PD were obtained as shown in Fig. 11. It is clearly indicated that errors in the image edges are larger than those in the image center.

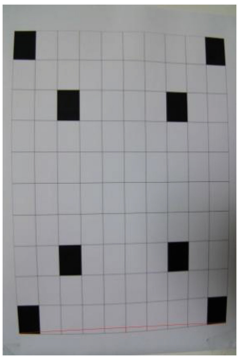

Fig. 8. The original image

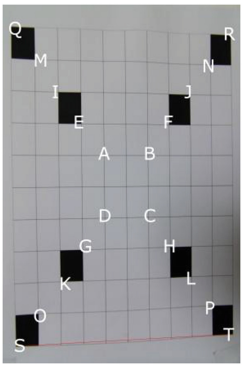

Fig. 9. The corrected image

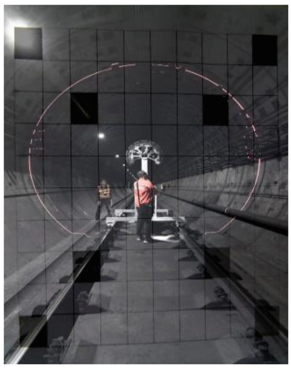

Fig. 10. The outline range

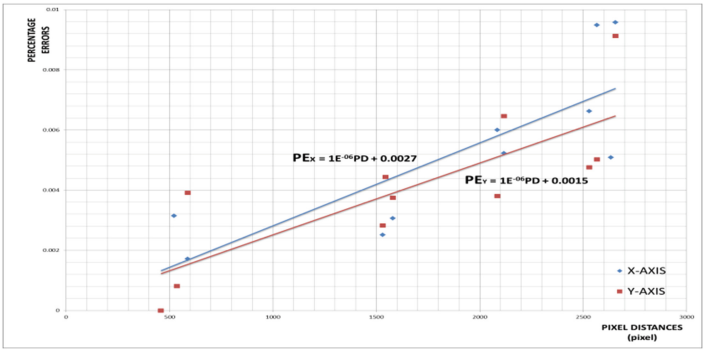

Fig. 11. The curve of percentage errors to pixel distances

3.2 Field Experiment

A series of tests were carried out in the subway tunnel of Shanghai Metro Line 1 using the specially-designed device. Specific experiment steps were as follows: (1) The laser range-finder and the protractor were installed on the tunnel inspection vehicle. (2) The laser source was powered and it formed a bright red circular outline on the inner surface of the lining. (3) The laser range-finder was rotated with a 10-degree interval. (4) The real-time distances and their corresponding angles were recorded. (5) During the test, a total station was used to get the precise coordinates of these recorded points.

The model of the inspection device was MTI-200A (see Fig. 10). The laser range-finder's model was HZH-80 with an accuracy of 1 mm. The total station's model was SOKKIA CX-102. Its accuracy was (3 + 2 ppm*D) mm without reflection prism.

3.3 Test Results

Pixel coordinates of tens of thousands of target points on the outline were extracted automatically on the basis of color differences using Mathematica software. In total, about seventeen thousand pixel points were extracted of each outline.

Twenty uniformly-distributed control points were taken into consideration. Two fitting outlines are shown in Fig. 12. The red one was fitted based on the absolute coordinates measured by the total station while the blue one was fitted according to the data obtained by the proposed method. The horizontal diameter of the red outline was 5539 mm whereas that of the blue one was 5533 mm, meaning that the error was below 6 mm.

According to the design document as Fig. 13 shows, the designed dimension of the tunnel's inner diameter was 5500 mm. The maximum magnitude of horizontal convergence was around 39 mm, which was in accordance with the monitoring data on site.

Compared with the total station, the precision of the proposed method was acceptable and the method was more flexible and more effective. The specially-designed mobile device was not only low-cost but also handy. With the device, the DLT method was potential to be applied in tunnel deformation monitoring. The abundant measurement results would provide basing data for stress analysis and performance analysis.

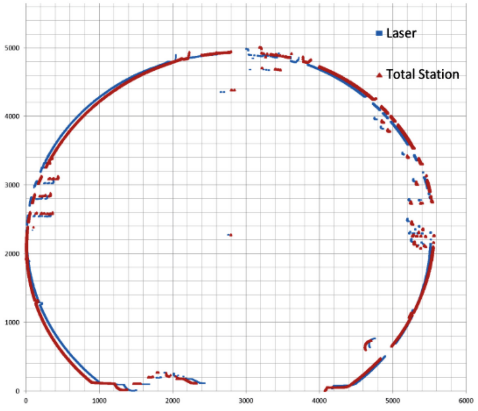

Fig. 12. Two fitting outlines (Color figure online)

3.4 Discussion

As Fig. 12 shows, there are still some deviations between the red outline and the blue one. Error sources in close range photogrammetry were discussed thoroughly by Song et al. (2010) [20]. In this test, there were various factors that led to errors. They were analyzed as follows: (1) The image distortion still had a little influence on the results. (2) The laser range-finder was rotated manually, leading to inaccuracy in angles. (3) The measuring equipment had systemic errors. (4) The sensor's pixels were not abundant enough.

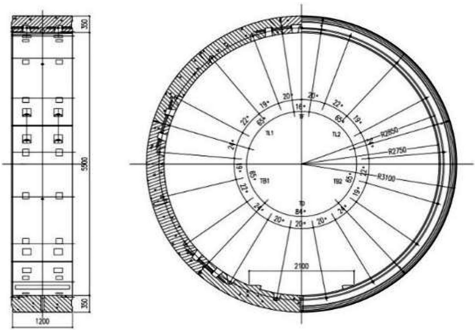

Fig. 13. The geometry of shield tunnel's linings

More control points will lead to higher measuring precision intuitively. However, it means a higher cost meanwhile. The optimal option should satisfy the precision requirements at minimum costs. An important question is determining that how many control points are optimal.

Assuming that eight control points are optimal, then eight laser range-finders are installed uniformly on a protractor. It is fixed on the inspection device in practical applications. When the device moves along the tracks, the only thing necessary is to photograph the outline continually. Each photo records a certain outline and hundreds of outlines are recorded. Photoelectric encoder is used to record the real-time distances the device has moved. Once the outlines and their corresponding locations are combined correctly, the complete 3D shape of a tunnel will be gained, which is extremely helpful for engineers to evaluate the tunnel's performance.

4 Conclusions

A novel method for measuring tunnel cross sections was put forward. It was based on laser orientation module, laser range-finding module and the theory of close range photogrammetry. A series of tests in the subway tunnel of Shanghai Metro Line 1 were carried out to validate the method being low-cost and precise. Measurement results were satisfied with twenty uniformly-distributed control points for the tunnel around 5.5 m in diameter. The maximum error between the calculated outline and the actual outline was just 6 mm.

Acknowledgements. The authors acknowledge the support of National Natural-Science Foundation of China (Grant No. 40772179), Science and Technology Commission of Shanghai Municipality (Grant No. 16DZ1200402) and the support of Science and Technology Plan of Department of Communication of Zhejiang province (Grant No. 2010H29).

References

1. Wang, R.L.: Analysis on influencing factors and deformation characteristics of shanghai soft soil subway tunnel deformation. Undergr. Eng. Tunn. **1**(1), 7 (2009)
2. Zhang, D.M., Zou, W.B., Yan, J.Y.: Effective control of large transverse deformation of shield tunnels using grouting in soft deposits. Chin. J. Geotech. Eng. **36**(12), 2203–2212 (2014)
3. Bassett, R., Kimmance, J., Rasmussen, C.: An automated electrolevel deformation monitoring system for tunnels. Proc. Instit. Civil Eng. Geotech. Eng. **137**, 117–125 (1999)
4. Hope, Colin, Marcelo, C.: Geotechnical instrumentation news-manual total station monitoring. Geotech. News **26**(3), 28 (2008)
5. Yang, S.L., Wang, B., Ji, S.Y., Liu, W.N., Shi, H.Y.: Non-contact monitoring and analysis system for tunnel surrounding rock deformation of underground engineering. Trans. Nonferrous Met. Soc. China (English Edition) **15**, 88–91 (2005)
6. Yang, S., Liu, W., Shi, H., Huang, F.: A study on the theory and method of non-contact monitoring for tunnel rock deformation based on free stationing of a total station. China Civil Eng. J. **39**, 100–104 (2006)
7. Han, J.Y., Guo, J., Jiang, Y.S.: Monitoring tunnel profile by means of multi-epoch dispersed 3-D LiDAR point clouds. Tunn. Undergr. Space Technol. **33**, 186–192 (2013)
8. Xie, X.Y., Lu, X.Z.: Development of a 3D modeling algorithm for tunnel deformation monitoring based on terrestrial laser scanning. Undergr. Space **2**, 16–29 (2017)
9. Argüelles-Fraga, R., Ordóñez, C., García-Cortés, S., Roca-Pardiñas, J.: Measurement planning for circular cross-section tunnels using terrestrial laser scanning. Autom. Constr. **31**(3), 1–9 (2013)
10. Ethrog, U., Shmutter, B.: Tunnel calibration by photogrammetry. Photogrammetria **38**(3), 103–113 (1982)
11. Zhang, Q.F., Hang, Y.X., Yang, H.B.: Area measurement of irregular plane object using area array CCD. Instrum. Tech. Sens. **2**, 36–39 (2000)
12. Yang, L.F., Hang, J.W., Li, Y.Z.: Application of high resolution measurement technique with area CCD. J. Taiyuan Univ. Technol. **32**(5), 455–458 (2001)
13. Lee, Y.J., Bassett, R.H.: Application of a photogrammetric technique to a model tunnel. Tunn. Undergr. Space Technol. **21**(1), 79–95 (2006)
14. Hu, T.Y.: Study on Close Range Photogrammetry in Tunneling Engineering's Application. Beijing Jiaotong University, Beijing (2008)
15. Chen, Z.H., Zhao, M., Qiao, D.L.: Research on monitoring method of metro tunnel deformation based on close - range photogrammetry. Spec. Struct. **5**, 61–65 (2014)
16. Abdel-Aziz, Y.I., Karara, H.M.: Direct linear transformation from comparator coordinates into object space coordinates in close-range photogrammetry. Photogramm. Eng. Remote Sens. **81**, 103–107 (2015)
17. Ma, G.L., Zhang, Q.Y., Li, S.C.: Application of digital photogrammy in deformation measurement for 3D geo-mechanics model test of large tunnel driving. J. Geotech. Investig. Surv. **6**, 50–52 (2006)
18. DXOMARK. http://www.dxomark.com
19. Jin, Y., Meng, J.B., Wang, K.: The research of plane array camera geometric distortion correction method. Microelectron. Comput. **28**(10), 36–38 (2011)
20. Song, M.: Analysis on precision of multi-lens area array CCD mapping camera. Chin. J. Space Sci. **30**(6), 589–595 (2010)